

# A Spatial Multi-Cellular Model of the Pancreatic Islet including $\alpha$ -, $\beta$ -, and $\delta$ -cells

REU Site: Interdisciplinary Program in High Performance Computing

Annie Dai<sup>1</sup>, David Palensky<sup>2</sup>, Alex Piatski<sup>3</sup>, Kendall Queen<sup>4</sup>, Gina Vockeroth<sup>5</sup>,  
Graduate assistant: Teresa Lehair<sup>6</sup>, Faculty mentor: Bradford E. Percy<sup>6</sup>,  
Clients: Margaret Watts<sup>7</sup> and Arthur Sherman<sup>7</sup>

<sup>1</sup>Department of Mathematics, Northeastern University

<sup>2</sup>Department of Mathematics, University of Maryland, College Park

<sup>3</sup>Department of Computer and Information Science, University of Pennsylvania

<sup>4</sup>Department of Computer Science and Electrical Engineering, UMBC

<sup>5</sup>Department of Mathematics and Statistics, Loyola University Chicago

<sup>6</sup>Department of Mathematics and Statistics, UMBC

<sup>7</sup>Laboratory of Biological Modeling, National Institutes of Health

Technical Report HPCF-2014-13, [www.umbc.edu/hpcf](http://www.umbc.edu/hpcf) > Publications

## Proposal

Our goal is to create a computational model of an islet of Langerhans, consisting of  $\alpha$ -,  $\beta$ -, and  $\delta$ -cells. We will focus on varying the geometries and proportions of the cells in this islet, and study the hormonal secretion and reception of each cell at any point in time. We are currently considering basic cubic and spherical models, among others. Besides changing the physical shape of our islet, we will change the sequential ordering of the cell types in our model.

We will have three different models (one for each cell type). While  $\beta$ -cells are already electronically wired,  $\alpha$ -cell and  $\delta$ -cell paracrine interactions depend on a spatial-temporal model. We will use ODEs to model the behavior of these cells. We will use a diffusive PDE equation to model the propagation of the secretions (0.1). Out of computational concerns, we will hope to find and assume parameters that would allow us to use an analytical solution to the diffusive PDE. Currently, we are contemplating using the heat kernel to approximate a solution to (0.2). However, if such an approximation cannot be realized, we may just end up numerically solving the PDE's despite of the increase in computational complexity.

$$\frac{\partial u}{\partial t} - D\nabla^2 u = f(u, t) \quad (0.1)$$

$$K(t, x, y) = \frac{1}{(4\pi Dt)^{3/2}} e^{-|x-y|^2/4Dt} \quad (0.2)$$

Upon creating a modeling tool, we will be able to model experimental scenarios with similar geometries and proportions to human and mouse islets given in your presentation. We hope to simulate a core and mantle geometry for the mouse model by creating a core of  $\beta$ -cells with an  $\alpha$  and  $\delta$  mantle. We will see which geometries work best for such a simulation. Afterward, we will be prepared to compare our results to experimental data (already done by the NIH). We will also be able to use these models to isolate specific cell types and compare them to

each other at different points in the model, while toggling certain secretions — or any system parameter — to test if any paracrine interactions tame heterogeneity.

## 1 Introduction

Diabetes is a metabolic disorder that is characterized by high blood glucose levels. Type I diabetes is a result of destroyed  $\beta$ -cells which renders the body unable to produce insulin in order to effectively decrease blood glucose levels. Type II diabetes occurs when the body becomes resistant to insulin. The percentage of the population that is affected by diabetes rose from 8.3% in 2010 to 9.3% in 2012, or 25.8 million to 29.1 million respectively [1].

The cells responsible for the regulation of blood glucose are found in the pancreas in islets of Langerhans. These islets contain five types of cells; however, we only study  $\alpha$ -,  $\beta$ -, and  $\delta$ -cells.  $\beta$ -cells experience voltage oscillations when glucose is introduced. This is due to calcium entering the cell, which results in insulin release.  $\alpha$ -cells secrete glucagon, which rises when blood glucose levels are low, and is regulated by insulin and somatostatin.  $\delta$ -cells secrete somatostatin, which inhibits  $\alpha$ - and  $\beta$ -cells.

We are interested in modeling islets comprised of these cells in order to further understand paracrine interactions between them. In order to accomplish this we extend a previous Tri-Hormone Model, which simulates the interactions between one of each cell type. This model simulates the interaction of a  $\delta$ -cell with a  $\alpha$ - and  $\beta$ -cell by allowing the somatostatin to suppress insulin and glucagon through GIRK channels. It also simulates the interaction of  $\beta$ -cells with  $\alpha$ - and  $\delta$ -cells by allowing insulin to inhibit glucagon secretion through  $K(ATP)$  channels. These interactions take place within a common space in the islet. This simulation concluded that paracrine interactions are able to suppress  $\alpha$ -cells that secrete inappropriately when cell types are distributed on a bell-shaped curve [5].

Our model scales this Tri-Hormone Model into a  $N \times N \times N$  cube with the capability of choosing the cell type arrangement. We incorporate  $\beta$ -cell coupling and model the behavior between  $\alpha$ - and  $\delta$ -cells as diffusive.  $\alpha$ - and  $\delta$ -cells do not communicate via gap junctions, thus their secretion is treated as heat diffusion. We model this secretion by

$$\frac{\partial u}{\partial t} - D\nabla^2 u = f(u, t) \tag{1.1}$$

For our computational model we implement a system of twenty-six, twenty-three, and twenty-one ordinary differential equations for  $\alpha$ -,  $\beta$ -, and  $\delta$ -cells, respectively. To further comprehend how these cells interact in space we measure the rate of change for variables such as voltage, calcium, and the hormone that is secreted by each cell.

We simulate more realistic islets by looking at varying distributions and arrangements of  $\alpha$ -,  $\beta$ -, and  $\delta$ -cells. We look at four different cases which display the interactions in a cubic model arranged in three planes of each type of cell. Then we compare this with a mouse islet cell distribution, which accurately depicts the observed percentages of  $\alpha$ -,  $\beta$ -, and  $\delta$ -cells in a mouse islet. We compare this to our three-plane distribution in order to measure the difference in secretion in space for different cell distributions.

## 2 Background

The endocrine component of the pancreas is made up of groups of hormone-releasing cells called islets of Langerhans. These clusters are made up of individual  $\alpha$ -,  $\beta$ -, and  $\delta$ -cells. The  $\alpha$ -cells secrete glucagon, a hormone that increases blood glucose levels. To lower glucose levels,  $\beta$ -cells release insulin. Finally, when levels are high,  $\delta$ -cells secrete somatostatin to regulate the  $\alpha$ -cell and  $\beta$ -cell secretions.

Diabetics have issues with insulin secretion. In type I diabetes, an autoimmune attack results in destroyed  $\beta$ -cells leaving the body with an inability to produce insulin. Type II diabetes pertains more to the body's resistance to insulin than the destroyed  $\beta$ -cells. Statistics indicate that 25.8 million people suffer from diabetes [cite]. As a result, the study of pancreatic islets is an area of scientific research. A computational model to simulate  $\alpha$ -,  $\beta$ -, and  $\delta$ -cell paracrine interaction could provide the field with faster and more accurate methods of modeling paracrine interactions to aid diabetic research. Upon the creation of such a tool, scientists will no longer be limited to human simulations. Comparisons and cross studies of those could be made with in-vivo mice as well.

A main difference between rodent and human islets is the respective percentages of  $\alpha$ -,  $\beta$ -, and  $\delta$ -cells. In rodent islets,  $\beta$ -cells compose 60-80% of the total cell population,  $\alpha$ -cells make up about 15-20%, and  $\delta$ -cells account for less than 10%. In human islets,  $\beta$ -cells make up 48-59% of the total amount of cells,  $\alpha$ -cells compose about 33-46%, and  $\delta$ -cells make up less than 20% [3].

Another difference between rodent and human islets is the spatial distribution of  $\alpha$ -,  $\beta$ -, and  $\delta$ -cells. In rodents, the core of an islet is made up of  $\beta$ -cells, and the mantle is composed of  $\alpha$ - and  $\delta$ -cells. In contrast, human islets have a more disorganized cell population distribution in which most  $\beta$ -cells are next to  $\alpha$ - and  $\delta$ -cells. An additional difference between rodent and human islets is the intercellular communication occurring in  $\beta$ -cell populations via electrical coupling. In rodents the  $\beta$ -cells perform their electrical coupling as a syncytium. However, in human islets electrical coupling occurs between  $\beta$ -cells in the same islet, but not between  $\beta$ -cells located in different islets. [3].

Section 2.1 describes a general model of the paracrine interactions between the three cell types. Section 2.2 provides the physiology and mathematical models behind each paracrine interaction in the tri-hormonal model. Section 2.3 provides a description of the 2013 REU's group's project's relevance to ours. Section 2.4 provides the mathematical models we use to simulate cell behavior and interaction in our computations.

### 2.1 Tri-Hormone Model

A Tri-Hormone Model can be efficiently used to simulate paracrine interaction. Such a model consists of one  $\alpha$ -, one  $\beta$ -, and one  $\delta$ -cell. REFERENCE TABLES HERE Each cell secretes into a closed space, and all cells are influenced by this secretion. To further simplify the computation, scientists ignore diffusion and neglect all spatial components. As a result, at the time a molecule is secreted, all cells in the system feel it instantaneously. The following equation models insulin secretion:

$$\frac{dIns_{comp}}{dt} = \frac{ISR}{v_{comp}} - f_{comp,b}Ins_{comp} \quad (2.1)$$

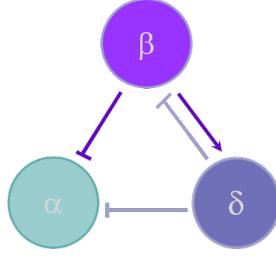


Figure 2.1: Tri-Hormone Model

In the Tri-Hormone Model, there exist four main paracrine interactions: 1.)  $\beta$ -cell inhibiting  $\alpha$ -cell (glucagon) secretion. 2.)  $\beta$ -cell stimulating  $\delta$ -cell secretion. 3.)  $\delta$ -cell inhibiting  $\beta$ -cell secretion. 4.)  $\delta$ -cell inhibiting  $\alpha$ -cell secretion [6]. See Figure 2.1 [5].

## 2.2 Physiology behind Paracrine Interactions in a Tri-Hormonal Model

The Tri-Hormone Model is a direct representation of small-scaled interactions between  $\alpha$ -,  $\beta$ -, and  $\delta$ -cells. Analyzing the tri-cell model can lead to the development of a full-scale model. The following sections will explain how each type of cell works together and interacts with each other thus creating the effect of a pancreatic islet.

### 2.2.1 The $\beta$ -cell inhibition of $\alpha$ -cell secretion

Insulin inhibits  $\alpha$ -cell secretion by opening  $K(ATP)$  channels. This is modeled by the following equations:

$$EffIa = \frac{0.006}{1 + \exp\left(\frac{-Ins+100}{40}\right)} + 0.04 \quad (2.2)$$

$$g(KATP)a = \overline{gK(ATP)a} \cdot EffI \quad (2.3)$$

It is important to note that  $EffI$  is the amount of insulin in the secreted space. Also, as  $K(ATP)$  channels increase,  $gK(ATP)$  increases as well. An increase in  $gK(ATP)$  usually causes a decrease in glucagon secretion [6].

### 2.2.2 The $\beta$ -cell stimulation of $\delta$ -cell secretion

To create the stimulatory effect that relates  $\beta$ - and  $\delta$ -cell secretions, an inward GABA CL channel is used. This can be done because GABA is secreted alongside insulin, so GABA's effect can be modeled based on the  $\beta$ -cell's release of insulin [6]. The following equation is used to model this effect:

$$EffId = \frac{0.8}{1 + \exp\left(\frac{-Ins+150}{50}\right)} \quad (2.4)$$

### 2.2.3 The $\delta$ -cell inhibition of $\beta$ -cells

The way  $\delta$ -cells inhibit  $\beta$ -cells is through G protein inwardly rectifying potassium (GIRK) channels [6]. This is modeled as if it is a K channel.

$$EffId = \frac{1}{1 + \exp\left(\frac{-Som+10}{10}\right)} \quad (2.5)$$

$$IGIRKb = 10EffIS(Vb - (-80)) \quad (2.6)$$

### 2.2.4 The $\delta$ -cell inhibition of $\alpha$ -cells

The inhibition of  $\alpha$ -cells is a bit more interesting. Along with GIRK channel inhibition,  $\delta$ -cells de-prime granules to inhibit  $\alpha$ -cells [6]. This is modeled by the following equation, which correlates secretion with the rate of change in granules as somatostatin increases.

$$r_{-2a} = \frac{5}{1 + \exp(-Som + 20)} \quad (2.7)$$

## 2.3 Physiology of $\alpha$ -cell and $\beta$ -cell Secretion

With today's diabetes research, scientists, doctors, and researchers can better understand how our body works, the causes of type 1 and type 2 diabetes, and the inner workings of human pancreatic functions. Through previous work the research community has found that the endocrine part of the pancreas contains clusters of cells called islet of Langerhans [2]. Though these islets house many cells, a focus was taken by Team 4 (2013) in exploring the  $\beta$ -cell's functionality and modeling the physiology of the  $\beta$ -cell [2]. The  $\beta$ -cell's physiology is highly characterized by voltage and calcium oscillations that correlate with insulin secretion [2]. Inside the islet of Langerhans,  $\beta$ -cells are connected to each other via gap junctions, which are intercellular connections. Within gap junctions, small ions and products of metabolism, called metabolites, are free to flow between the cells. Research shows that metabolites influence the oscillations found in  $\beta$ -cells causing insulin secretion [2].

"Voltage and metabolites, such as glucose 6-phosphate (G6P) and fructose 1-6-bisphosphate (FBP)," undergo oscillations when glucose concentration increases in the bloodstream [2]. ADD FIGURES Glucose then enters the  $\beta$ -cell through glucose transporters, protein channels in the cell membrane that use diffusion as transportation. Once the cell metabolizes it produces adenosine triphosphate (ATP). Increases in the concentration of ATP triggers depolarization of  $\beta$ -cell membranes by closing channels of ATP-sensitive (KATP) channels, which causes calcium to enter the cell [2]. Due to the heightened concentration of calcium, the cell vesicles release insulin into the bloodstream. As insulin increases its presence in the bloodstream, glucose levels begin to decrease, causing a  $\beta$ -cell reset [2].

Previous numerical models have included an individual  $\beta$ -cell model and a tri-cell model of  $\alpha$ -,  $\beta$ -, and  $\delta$ -cells. The  $\beta$ -cell model was a system of seven coupled ordinary differential equations (ODEs) [2].

As discussed in Dr. Margaret Watts's and Dr. Arthur Sherman's published report, *Modeling the Pancreatic  $\alpha$ -Cell: Dual Mechanisms of Glucose Suppression of Glucagon Secretion*,  $\alpha$ -cell machinery is very similar to that of  $\beta$ -cells. Glucose transporters, voltage-gated  $Ca^{2+}$

channels, and  $K(\text{ATP})$  channels are all present, and behave similarly in  $\alpha$ -cell secretion. However, looking past this basic machinery, the advanced mechanisms of glucagon secretion are not very well understood. Currently, two major theories exist.

One theory claims that glucose directly suppresses glucagon secretion through intrinsic mechanisms [4]. The claim theorizes that glucose affects the  $\alpha$ -cell through closure of  $K(\text{ATP})$  channels. Just like in  $\beta$ -cells, this would result in an increase in the ATP/ADP ratio, and a closure of  $K(\text{ATP})$  channels and cell depolarization [4]. However, unlike in  $\beta$ -cells, this is actually theorized to cause a decrease in glucagon secretion.

The other theory claims that, instead of focusing on  $K(\text{ATP})$ , glucose affects glucagon secretion through a store-operated current (SOC) [4]. Glucose does this by providing additional ATP to activate the sarcoenoplasmic reticulum calcium transport ATPase (SERCA). SERCA would pump and fill calcium stores, which would as a result decrease secretion [4]. In contrast, when glucose levels decrease, calcium stores empty, SOC is turned on, and glucagon secretion increases. Overall, while the machinery is similar to that of insulin secretion in  $\beta$ -cells, the theorized process is rather different. All  $\alpha$ -cell models can be found in Tables (insert label once we figure it all out).

## 2.4 Tables

Table 2.1: Voltage Equations

Cell Type	Equation
$\alpha$	$\frac{dV}{dt} = -\frac{I_{\text{Cal}} + I_{\text{Cat}} + I_{\text{Capq}} + I_{\text{Na}} + I_{\text{Kdr}} + I_{\text{K(ATP)}} + I_{\text{Kaa}} + I_{\text{L}} + I_{\text{Soc}} + I_{\text{Som}}}{C_m}$
$\beta$	$\frac{dV}{dt} = -\frac{I_{\text{K}} + I_{\text{Ca}} + I_{\text{K(Ca)}} + I_{\text{K(ATP)}} + I_{\text{Som}}}{C_m}$
$\delta$	$\frac{dV}{dt} = -\frac{I_{\text{Cal}} + I_{\text{Cat}} + I_{\text{Capq}} + I_{\text{Na}} + I_{\text{Kdr}} + I_{\text{K(ATP)}} + I_{\text{Ka}} + I_{\text{L}} + I_{\text{Soc}} + I_{\text{Ins}}}{C_m}$

Table 2.2: Current Equations

Type of Current	$\alpha$	$\beta$	$\delta$
$I_k =$	N/A	$g_k n(v - v_k)$	N/A
$I_{ca} =$	N/A	$g_{ca} n_{ca} m_{\infty}(v - v_{ca})$	N/A
$I_{kca} =$	N/A	$\frac{g_{kca}}{1 + \frac{k_d}{c}}(v - v_k)$	N/A
$I_{katp} =$	$g_{katp}(v - v_k)$	$(1 - D_z)(g_{katp} katpo(v - v_k)) + (1 - D_z)(g_{katp}(v - v_k))$	$g_{katp}(v - v_k)$
$I_{cal} =$	$g_{cal} m_{cal}^2 h_{cal}(v - v_{ca})$	N/A	$g_{cal} m_{cal}^2 h_{cal}(v - v_{ca})$
$I_{cat} =$	$g_{cat} m_{cat}^3 h_{cat}(v - v_{ca})$	N/A	$g_{cat} m_{cat}^3 h_{cat}(v - v_{ca})$
$I_{capq} =$	$g_{capq} m_{capq} h_{capq}(v - v_{ca})$	N/A	$g_{capq} m_{capq} h_{capq}(v - v_{ca})$
$I_{na} =$	$g_{na} m_{na}^3 h_{na}(v - v_{na})$	N/A	$g_{na} m_{na}^3 h_{na}(v - v_{na})$
$I_{ka} =$	$g_{ka} m_{ka} h_{ka}(v - v_{ka})$	N/A	$g_{ka} m_{ka} h_{ka}(v - v_{ka})$
$I_{kdr} =$	$g_{kdr} m_{ka}^4(v - v_{ka})$	N/A	$g_{kdr} m_{ka}^4(v - v_{ka})$
$I_l =$	$g_l(v - v_l)$	N/A	$g_l(v - v_l)$
$I_{soc} =$	$g_{soc} c_{\infty}(v - v_{soc})$	N/A	$g_{soc}(v - v_{soc})$
$I_{som} =$	$g_{som} som_{\infty}(v - v_{som})$	$g_{som} som_{\infty}(v - v_{som})$	N/A
$I_{ins} =$	N/A	N/A	$g_{ins} ins_{\infty}(v - v_{ins})$

Table 2.3: M Gating Variable Equations

Variable	Equation
$m'_j =$	$\frac{m_{j\infty} - m_j}{\tau_j}$
$m_{j\infty} =$	$\frac{1}{1 + e^{\frac{-(v-v_j)}{s_j}}}$
$\tau_j =$	$\frac{a}{e^{\frac{-(v+b)}{c}} + e^{\frac{v+b}{c}}} + d$

Table 2.4: Gating Variable Equations

j label	$\alpha$	$\beta$	$\delta$
$cal =$	$a = 1 \ b = 23 \ c = 20 \ d = 0.05$	N/A	$a = 1 \ b = 23 \ c = 20 \ d = 0.05$
$cal =$	$a = t_{cat1} \ b = 50 \ c = 12 \ d = t_{cat2}$	N/A	$a = t_{cat1} \ b = 50 \ c = 12 \ d = t_{cat2}$
$capq =$	$a = 1 \ b = 50 \ c = 12 \ d = 0.05$	N/A	$a = 1 \ b = 50 \ c = 12 \ d = 0.05$
$na =$	$a = 6 \ b = 50 \ c = 10 \ d = 0.05$	N/A	$a = 6 \ b = 50 \ c = 10 \ d = 0.05$
$ka =$	$\tau_{ka} = 0.1$	N/A	$\tau_{ka} = 0.1$
$kdr =$	$a = 1.5 \ b = 10 \ c = 25 \ d = 15$	N/A	$a = 1.5 \ b = 10 \ c = 25 \ d = 15$

Table 2.5: H Gating Variable Equations

Variable	Equation
$h'_j =$	$\frac{h_{j\infty} - h_j}{\tau_j}$
$h_{j\infty} =$	$\frac{1}{1 + e^{\frac{-(v-v_j)}{s_j}}}$
$\tau_j =$	$\frac{a}{e^{\frac{-(v+b)}{c}} + e^{\frac{v+b}{c}}} + d$

Table 2.6: H tables

j label	$\alpha$	$\beta$	$\delta$
$cal =$	$a = t_{cal1} \ b = 0 \ c = 20 \ d = t_{cal2}$	N/A	$a = t_{cal1} \ b = 0 \ c = 20 \ d = t_{cal2}$
$cat =$	$a = t_{cat1} \ b = 50 \ c = 15 \ d = t_{cat2}$	N/A	$a = t_{cat1} \ b = 50 \ c = 15 \ d = t_{cat2}$
$capq =$	$a = t_{capq1} \ b = 50 \ c = 10 \ d = t_{capq2}$	N/A	$a = t_{capq1} \ b = 50 \ c = 10 \ d = t_{capq2}$
$na =$	$a = t_{na1} \ b = 50 \ c = 8 \ d = t_{na2}$	N/A	$a = t_{na1} \ b = 50 \ c = 8 \ d = t_{na2}$
$ka =$	$a = t_{ka1} \ b = 5 \ c = 20 \ d = t_{ka2}$	N/A	$a = t_{ka1} \ b = 5 \ c = 20 \ d = t_{ka2}$

Table 2.7: J Tables

Type of J	$\alpha$	$\beta$	$\delta$
$J_L =$	$\frac{-\alpha I_{CaL}}{v_{cell}}$	$\frac{-\alpha I_{CaL}}{v_{md}}$	$\frac{-\alpha I_{CaL}}{v_{mdl}}$
$J_{PQ} =$	$\frac{-\alpha I_{Capq}}{v_{mdpq}}$	N/A	$\frac{-\alpha I_{Capq}}{v_{mdpq}}$
$J_T =$	$\frac{-\alpha I_{Cat}}{v_{cell}}$	N/A	$\frac{-\alpha I_{Cat}}{v_{cell}}$
$J_{serca} =$	$k_{serca}c$	$k_{serca2} + k_{serca3}c$	$k_{serca}c$
$J_{leak} =$	$p_{leak}(c_{er} - c)$	$p_{er}(c_{er} - c)$	$p_{leak}(c_{er} - c)$
$J_{er} =$	$J_{leak} - J_{serca}$	$\frac{eps_{er}(J_{leak} - J_{serca})}{\lambda_{er}}$	$\frac{eps_{er}(J_{leak} - J_{serca})}{\lambda_{er}}$
$J_R =$	N/A	$\frac{-\alpha I_{CaR}}{v_{cell}}$	N/A

Table 2.8:  $J_{mem}$

Cell Type	Equation
$\alpha$	$J_T + J_L + fV_{pq}B(c_{mdpq} - c - k_{pmca}c)$
$\beta$	$JR + vmdcytB(c_{md} - c) - k_{pmca}(c - c_{bas})$
$\delta$	$J_T + J_L + fV_{pq}B(c_{mdpq} - c - k_{pmca}c)$

### 3 Methodology

We have XPP code that implements a tri-cell model of an islet. We translate the XPP code into Matlab code. We then scale the original model in order to implement a model of an islet with more than one  $\alpha$ -,  $\beta$ -, and  $\delta$ -cell each.

#### 3.1 Extending Tri-hormonal Model

The Tri-Hormone Model consists of an islet with one of each cell type that secretes (instantaneously) into a shared space [6]. In order to extend this model from three cells to an accurate physiological islet, we partition each type of cell in Matlab so that each can be run through an ordinary differential equation (ode) solver. For  $\alpha$ -,  $\beta$ -, and  $\delta$ -cells we use functions of twenty-four, twenty-one, and nineteen differential equations, respectively. In order to simulate the Tri-Hormone model, we run each of these cell functions simultaneously. Each cells variables are solved and stored in order, from alpha to delta, into a matrix A that is  $N \times M$ , where  $N$  = the amount of time steps and  $M$  = the sum of the cell variables.

$$A = \begin{pmatrix} v_{\alpha t1} \dots Effg_{t1} v_{\beta t1} \dots Effi_{t1} v_{\delta t1} \dots Effs_{t1} \\ v_{\alpha t2} \dots Effg_{t2} v_{\beta t2} \dots Effi_{t2} v_{\delta t2} \dots Effs_{t2} \\ \vdots \quad \vdots \\ v_{\alpha tf} \dots Effg_{tf} v_{\beta tf} \dots Effi_{tf} v_{\delta tf} \dots Effs_{tf} \end{pmatrix}$$

To model various paracrine interactions, we add coupling parameters (in this case, in the form of currents) to our voltage equations. We repeat this process at each time step, using different parameters. This allows us to make a dynamic system of cells that are affected by the secreted hormones, as well as the cells' independent voltages. A key methodological implementation that we made was to de-vectorize the secretion that we pass into our functions. We observe the total amount of secretion that the cell receives, then sum all the values of a secreted hormone creating a scalar value used by our functions.

In order to implement our scaled model for more than one cell of each type, we vectorize our coupled islet function. Given a user input, the initial values for the differential functions are duplicated for each new cell implemented. Due to Matlab's compatibility with vector algebra, we can easily exchange our initial function parameters with vector values. We are considering three different distributions of a  $3 \times 3 \times 3$  cell islet with three contiguous planes of  $\alpha$ -,  $\beta$ -, and  $\delta$ -cells.

The  $\alpha$ ,  $\beta$ , and  $\delta$  functions are scaled by  $N_a$ ,  $N_b$ , and  $N_d$ , the number of cells per type respectively, where  $N_x$  is the number of cells. Each cells variables are then multiplied by the number of each cell type respectively. We can then look at the paracrine effects on a much larger scale with different distributions of each cell type.

#### 1 $N_a = N_b = N_d = 1$

This case is the Tri-Hormone Model explained earlier. We have a compartmentalized islet of 1 of each cell. We can compare this version to the XPP code provided by the NIH to ensure accuracy.

## 2 $N_a = N_b = N_d = 9$

This case observes the effect of the sum of somatostatin and insulin secretion on each cell in the islet at every time step.

## 3 $N_a = N_b = N_d = 9$

This case observes the case 1 islet but accounts for the average amount of somatostatin secreted by dividing the secreted sum by the number of cells secreting that value. In other words, the summed somatostatin is divided by the number of  $\delta$ -cells, and the summed insulin secretion by the number of  $\beta$ -cells. (In this case: 9)

## 4 $N_a = 5, N_b = 20, N_d = 2$

This case emulates the observed distribution of cells in a mouse islet (reference background of mouse islets). This case also keeps the division of the number of cells secreted, as in case 2, to account for the changing number of  $\beta$ - and  $\delta$ -cells.

### 3.1.1 Cell Coupling

In order to simulate  $\beta$ -cell coupling via gap junctions, we implement a matrix vector product that models the change in voltage in each cell. We duplicate a linear index representation of each cell [2]. We give each cell a  $(i, j, k)$  entry with  $i + (j - 1)N + (k - 1)N^2$  (show Annie's picture) in an  $N^3 \times N^3$  matrix.

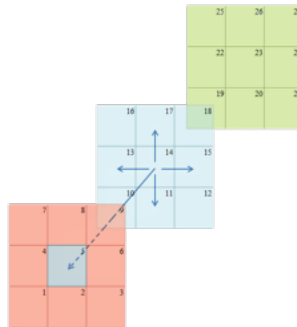


Figure 3.1: Example of Cell Coupling

For our  $3 \times 3 \times 3$  islet our coupling function places the three-dimensional positions of our  $\beta$  cells in a vector that is then transcribed into our coupling matrix. The  $(i, j)$  entry of the matrix represents the connection value for the  $i$ th and  $j$ th cell (either 0 or 1). For the  $i$ th cell in the matrix, our function sums the  $i$ th row, which represents the individual connections for one cell and stores this value in the  $(i, i)$  matrix. We take the product of our coupled matrix and our vector of  $\beta$ -cell voltages found at that time step via the ode solver. First, however, we must note that The 2013 REU's coupling matrix produces a  $N^3 \times N^3$  matrix which assumes that all cells in the system are  $\beta$ -cells.

	1	2	3	4	5	6	7	8	9	10	11	12	13	14	15	16	17	18	19	20	21	22	23	24	25	26	27
1	-3	1		1						1																	
2	1	-4	1		1						1																
3	1	-3			1							1															
4	1		-4	1		1							1														
5		1		1	-5	1		1						1													
6			1		1	-4		1							1												
7				1			-3	1								1											
8					1		1	-4	1								1										
9						1		1	-3										1								
10	1									-4	1		1						1								
11		1								1	-5	1		1						1							
12			1								1	-4			1						1						
13				1						1		-5	1		1							1					
14					1						1		1	-6	1		1						1				
15						1						1		1	-5			1						1			
16							1						1			-4	1								1		
17								1					1		1	-5	1									1	
18									1					1		1	-4										1
19										1									-3	1		1					
20											1								1	-4	1		1				
21												1								1	-3			1			
22													1						1			-4	1		1		
23														1						1		1	-5	1		1	
24															1						1		1	-4			1
25																1						1			-3	1	
26																	1						1		1	-4	1
27																		1						1		1	-3

Figure 3.2: Full Matrix

Given that our matrix does not consist of purely  $\beta$ -cells, we adjust the coupling matrix creating a new linear index of only the positions of  $\beta$ -cells in our system, and call this List B. We then index the original coupling matrix by omitting all rows and columns that are not a value in List B. We do this because the coupling is not affected by any row or column that represents a connection to an  $\alpha$ - or  $\delta$ -cell, since the electric coupling we are modeling only occurs within adjacent  $\beta$ -cells. We define adjacency as one unit away in the  $i$ ,  $j$ , or  $k$  direction. We then get a square matrix that has dimensions of the size of List B squared. Finally, we augment the diagonal values by assigning the value to the multiplicative inverse of the sum of all the representative connections in each row, representing the coupling of the remaining  $\beta$ -cells.

$$C = \begin{pmatrix} -2 & 1 & 0 & 1 & 0 & 0 & 0 & 0 & 0 \\ 1 & -3 & 1 & 0 & 1 & 0 & 0 & 0 & 0 \\ 0 & 1 & -2 & 0 & 0 & 1 & 0 & 0 & 0 \\ 1 & 0 & 0 & -3 & 1 & 0 & 1 & 0 & 0 \\ 0 & 1 & 0 & 1 & -4 & 1 & 0 & 1 & 0 \\ 0 & 0 & 1 & 0 & 1 & -3 & 0 & 0 & 1 \\ 0 & 0 & 0 & 1 & 0 & 0 & -2 & 1 & 0 \\ 0 & 0 & 0 & 0 & 1 & 0 & 1 & -3 & 1 \\ 0 & 0 & 0 & 0 & 0 & 1 & 0 & 1 & -2 \end{pmatrix} \quad V_b = \begin{pmatrix} v_1 \\ v_2 \\ v_3 \\ v_4 \\ v_5 \\ v_6 \\ v_7 \\ v_8 \\ v_9 \end{pmatrix}$$

The matrix above is the coupling matrix for a 3:3:3 model, which has 9 beta cells. Thus, it is 9x9. Our product represents a slight voltage change, which we add to our calculation of

dbdt. We do this in a similar fashion as with the other coupling functions, concatenation of a zero vector of placeholders with the vector of calculated  $\beta$  variables from the differential equations. This is also completed at every time step. To improve efficiency, the coupling matrix, and its indexed version, are calculated in the wrapper program before the main function and the ode solver are called. This can be done because once the amount and position of  $\beta$  cells are known, the coupling matrix stays constant, it is only the  $\beta$  voltage vector that changes every time step.

### 3.2 Secretion

Next we simulated the secretion of insulin, glucagon, and somatostatin molecules. We wanted to avoid doing an all-out partial differential equation (PDE) simulation, as it would severely slow our computational time. Instead, we decided to take advantage of our already discretized system, and treat the locations of the cells as points in space. We considered a standard diffusion problem:

$$s_t = \nabla \cdot (D\nabla s) + g(u(t))\delta(x) - ks, \quad -\infty < x, y, z < \infty \quad (3.1)$$

Here,  $g$  is a function of variables  $u$ , which is a function of time ( $t$ ). We will use  $\delta(x - x_1, y - y_1, z - z_1)$  to represent a  $\delta$  distribution, implying that the secretion is only produced at  $(x, y, z) = (x_1, y_1, z_1)$ . We rewrite this using a change of variables  $w = e^{kt}s$  to get

$$w_t = \nabla \cdot (D\nabla w) + G(u(t), t)\delta(x), \quad -\infty < x, y, z < \infty \quad (3.2)$$

Here,  $G(u, t) = e^{kt}g(u)$ . We can rewrite (3.2) as an analytical solution on an infinite domain:

$$w(x, y, z, t) = \int_0^t \frac{G(u(\tau), \tau)}{4\pi D(t - \tau)^{3/2}} e^{-\frac{((x-x_1)^2 + (y-y_1)^2 + (z-z_1)^2)}{4D(t-\tau)}} d\tau \quad (3.3)$$

We can rewrite this in terms of  $s$  (secretion) to get:

$$s(x, y, z, t) = \int_0^t \frac{g(u(\tau))}{4\pi D(t - \tau)^{3/2}} e^{-\frac{((x-x_1)^2 + (y-y_1)^2 + (z-z_1)^2)}{4D(t-\tau)}} d\tau \quad (3.4)$$

We now use a simple finite central difference approximation of the second order, instead of taking a limit derivative. In the single dimensional case  $S_x = \frac{\partial s(x,t)}{\partial(x)}$ . Thus we can approximate  $S_x \approx \frac{s(x+\delta x/2,t) - s(x-\delta x/2,t)}{\Delta x}$ . We use the same approximation for the second derivative, and get our diffusion equation!

$$S_{xx} = \frac{s(x + \Delta x, t) - 2s(x, t) + s(x - \Delta x, t)}{(\Delta x)^2} \quad (3.5)$$

We then extend this case to  $\mathbb{R}^3$  to get

$$\begin{aligned} \nabla \cdot (\nabla s) = & \frac{s(x + \Delta x, y, z, t) - 2s(x, y, z, t) + s(x - \Delta x, y, z, t)}{\Delta x^2} + \\ & \frac{s(x, y + \Delta y, z, t) - 2s(x, y, z, t) + s(x, y - \Delta y, z, t)}{\Delta x^2} + \\ & \frac{s(x, y, z + \Delta z, t) - 2s(x, y, z, t) + s(x, y, z - \Delta z, t)}{\Delta x^2} \end{aligned}$$

This diffusion approximation can now be calculated by passing in the full coupling matrix that was used by the 2013 REU, since we only care about the interaction between any adjacent cell, rather than just beta cells. Thus we get a new diffusion equation:

$$\hat{S}_t = \frac{D}{(\Delta x)^2} C \hat{s} + \hat{f} \quad (3.6)$$

Here, C is the full coupling matrix. The  $\hat{f}$  represents the initial secretion in to the system. For this example we will use  $\delta$ -cell somatostatin secretion. We have

$$\hat{f} = f(s, p) = \text{DeltaLoc} * \text{Effsfun} \quad (3.7)$$

Effsfun is a function that calculates the amount of effective (non-decayed) somatostatin that leaves a delta cell. It is then multiplied by Deltaloc- a binary vector of the same length as the linear ordering of the system. Deltaloc has 1's in the positions of  $\delta$ -cells, and 0's in the position of  $\alpha$  and  $\beta$ -cells. The multiplication of these two vectors results in a proper model of the initial somatostatin entering the system. An equivalent process is used for  $\alpha$ -cell glucagon and  $\beta$ -cell insulin-secretion.)

### 3.3 Paracrine Effects Taming Heterogeneity

In order to simulate the effects of paracrine coupling on the heterogeneity of alpha cells, we can assign two different  $G_{K(ATP)}$  values ( $26.5 * Dza + 0.04, 32 * Dza + 0.04$ ) to the alpha cells in our islet. This  $G_{K(ATP)}$  value is the conductance for the K(ATP) channel in the alpha cell, which varies depending on the amount of glucose in the blood. We simulate a high blood glucose level with our  $G_{K(ATP)} = 26.5 * Dza + 0.04$ . We will then run tests with and without the effects of beta and delta cells felt on alpha cells to see if paracrine coupling can tame the heterogeneity of alpha cells.

## 4 Results

All results have cell proportions (alpha:beta:delta).

### 4.1 Case 1: (1:1:1) Tri-Hormone Model

In order to check the accuracy of our Matlab code with the Tri-Hormone model in XPP, we first ran simulations of a three-cell islet, which contained one of each cell type. This is

modeled as a compartmental islet in which the secretion from each cell is felt instantaneously. Below in fig (1) we plot the voltages for each cell type in Matlab and compare them with the voltages for the XPP code. These voltages correspond with each cells secretion and we find similar oscillation patterns and timings for each. For a ten-minute simulation we observe that our alpha cell begins spiking around the 2 and 6 minute mark with a maximum and minimum amplitudes around 10 and -50 which is comparable to the XPP values. For the beta cell voltage in Matlab we notice oscillation spikes around the 2 and 6 minute mark, which corresponds to the voltage spikes in the XPP code. The beta cell values for the oscillations also correspond as we see the maximum and minimum from 10 to -40. We also see the voltages for the delta cell in Matlab experiences oscillation spikes from 2 to 5 minutes with maximum and minimum amplitude from about 0 to -50. These cell voltages give us confidence in that we were able to successfully re-create the Tri-Hormone in Matlab.

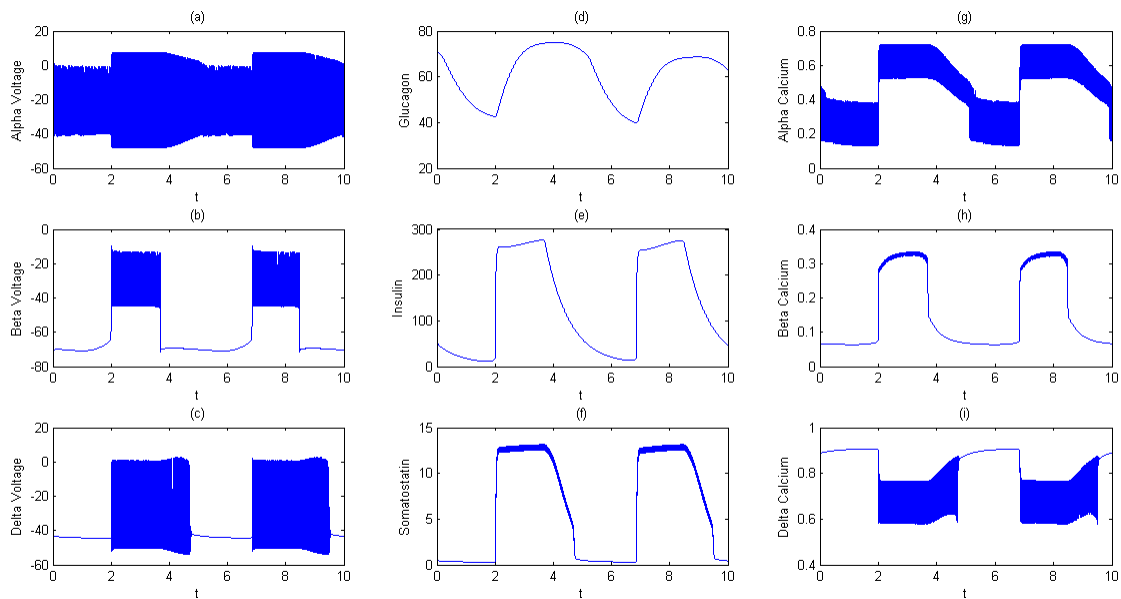


Figure 4.1: Tri-Hormone Model (1:1:1)

We also plotted the voltage of the islet.ode file that was provided by the NIH alongside our first case to show the similarities.

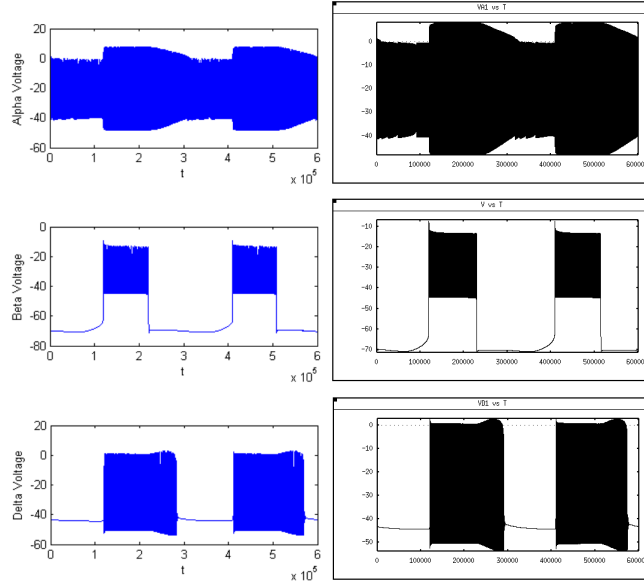


Figure 4.2: XPP/Matlab Compartmentalized Case 1 Comparison

## 4.2 Case 2: (9:9:9 Model with Summed Secretions)

In our second case we ran simulations on a  $3 \times 3 \times 3$  cubic islet with three sequential planes of nine cells for each cell type. For this case we applied the sum of somatostatin to each alpha and beta cell, as well as the sum of the insulin on each alpha and delta cell. This is done so that we can see the change in voltage when each cell is overwhelmed by the amount of hormone they receive. For a ten-minute simulation we see that the voltage for the alpha cell experiences large bursts for extended periods of 4 minutes (2-6 minutes) instead of 2 minute bursts that we saw in the Tri-Hormone model. Glucagon secretion also behaves differently in that it peaks at 77.5 at around the 2 minute mark and begins to decrease steadily until 10 minutes. This is in comparison to the Tri-Hormone simulations glucagon secretion which shows 5 minutes oscillations that range from 40 to 75. We also see a diminishing in the period for beta cell oscillation. The voltage oscillations exhibited in beta cells spike for less than two minutes ( $2 + x$  to  $4 - y$ ), which is in contrast to our Tri-Hormone model that displays oscillation spikes for 2 minutes. The delta cell in this summed simulation is in stark contrast to the delta cell of the Tri-Hormone model in that it oscillates for the entire 10 minutes instead of experiences non-oscillating periods. The delta cell also behaves differently in relation to somatostatin secretion. Somatostatin seems to be secreted at regular intervals of 5 minutes in comparison to the Tri-Hormone, which has periods of 2.5 minutes. The values at which somatostatin oscillates in this simulation range from 5 to 12.5 in comparison to 0 to 12.5 in the Tri-Hormone. Somatostatin is being released at a higher value throughout this simulation.

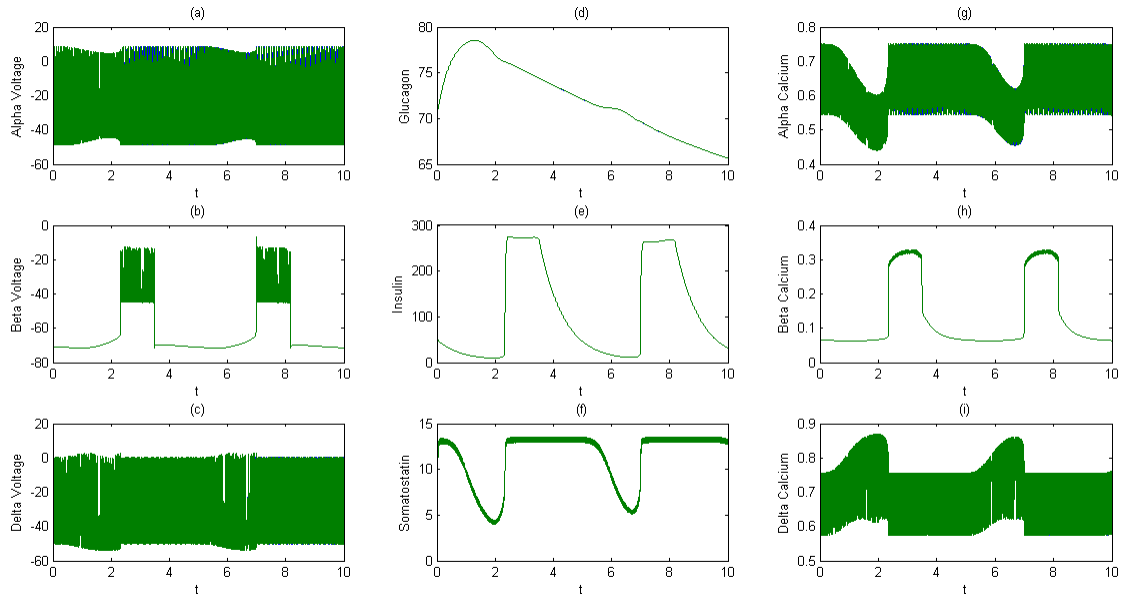


Figure 4.3: Compartmentalized Case 2

### 4.3 Case 3: (9:9:9 Model with Normalized Secretion)

In case 3 we ran simulations on the same islet as in case 2 however we varied the secretion values over the two cases. This case summed the amount of insulin detected by the alpha and delta cell and divided it by the number of beta cells (9). We also summed the amount of somatostatin that is secreted and detected by alpha and beta cells and divided the sum by the amount of delta cells. This is done so that each cell detects the average amount of secretion. When we average the secretion, the behavior of the alpha, beta and delta cells shifts back towards the behavior of the Tri-Hormone model. The voltage for the alpha cell shows maximum oscillations from 2-4 and 7-9 minutes from 10 to -50, just as in the Tri-Hormone model. The beta cell voltage also returns to the Tri-Hormone model behavior by showing oscillation spikes around the 2-4 and 7-9 minutes mark, with oscillations between 10 and -40. The voltage for the delta cell also exhibits maximum oscillations in the 2-5 and 7-9 minute marks, having oscillations between 0 and -50. Each of these cells behavior emulates the behavior shown in the Tri-Hormone model.

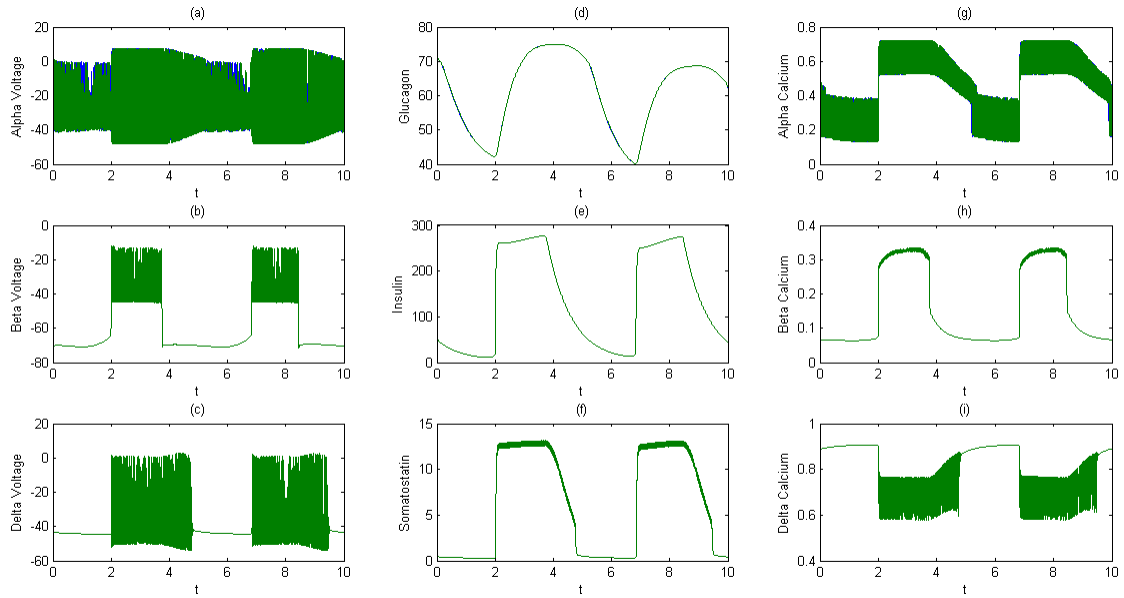


Figure 4.4: Compartmentalized Case 3

#### 4.4 Case 4: 5:20:2 Mouse Islet with Normalized Secretion

This case simulates a Mouse Islet cellular distribution for a  $3 \times 3 \times 3$  cube Islet. The amount of secretion is divided by 9 just as in case 3 in order to examine the effects that different cell distributions have on cell behavior. In this simulation we can notice a longer period of maximum oscillation for the voltage of alpha cells when compared to our averaged model. The range of oscillation is comparable however the period spans from 3 minutes (2-5 minute mark) instead of 2 minutes (2-4 minute mark). Glucagon behavior also differs slightly from the averaged model with values ranging from 50-75 instead of 40-75. Beta cell behavior remains constant with the averaged model. The voltages for beta cell exhibit bursts from 2-4 minutes and 7-9 minutes just as in the averaged model. Compared with our averaged model delta cell behavior has also changed. Delta cell voltage exhibit longer bursts from 2 minutes to just under 6 minutes (about 4 minutes) instead of about 3 minutes. There is also an initial burst in voltage at time 0 which we do not see in any other case. The somatostatin secretion also sees extended maximum bursts. We see somatostatin spike at 2 minutes from 0 to 12.5 for 3 minutes instead of 2 minutes as with our averaged model.

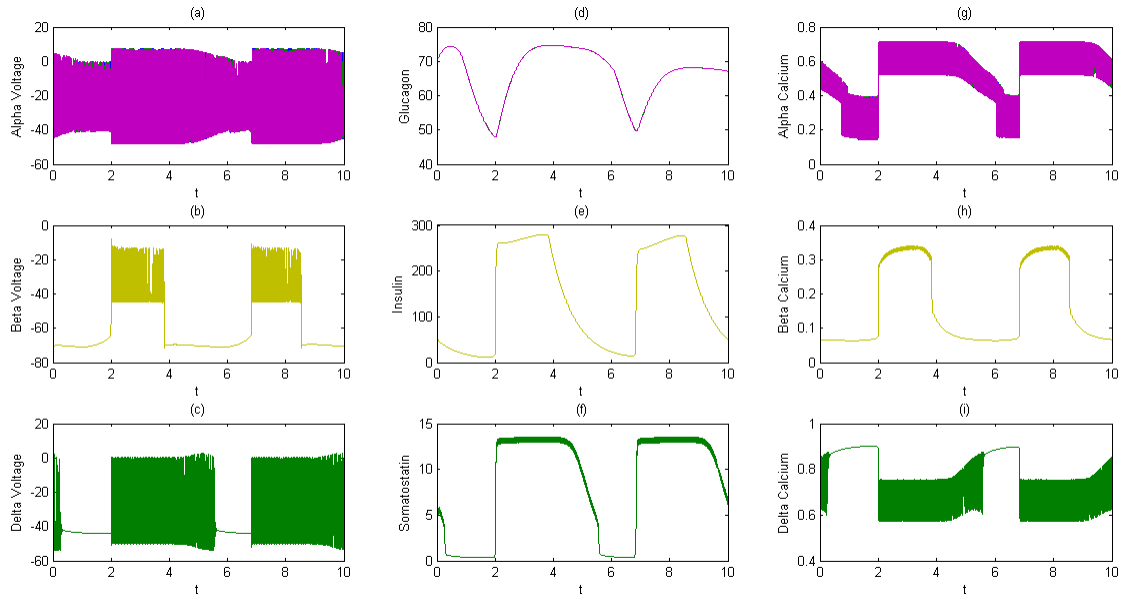


Figure 4.5: Compartmentalized Case 4

#### 4.4.1 Spatial Case 3

Upon the implementation of spatial coupling, we ran the equivalent cell distribution of the compartmentalized case 3 and 4. Below is the full data for Case 3. The amplitudes of the various values tend to be smaller than those in the compartmentalized model. This is probably because we are no longer passing in the full hormonal secretion values to each cell at each point. The secreted hormones are now spatial and time dependent, and with an added delay constant, result in smaller values at each discretized point.

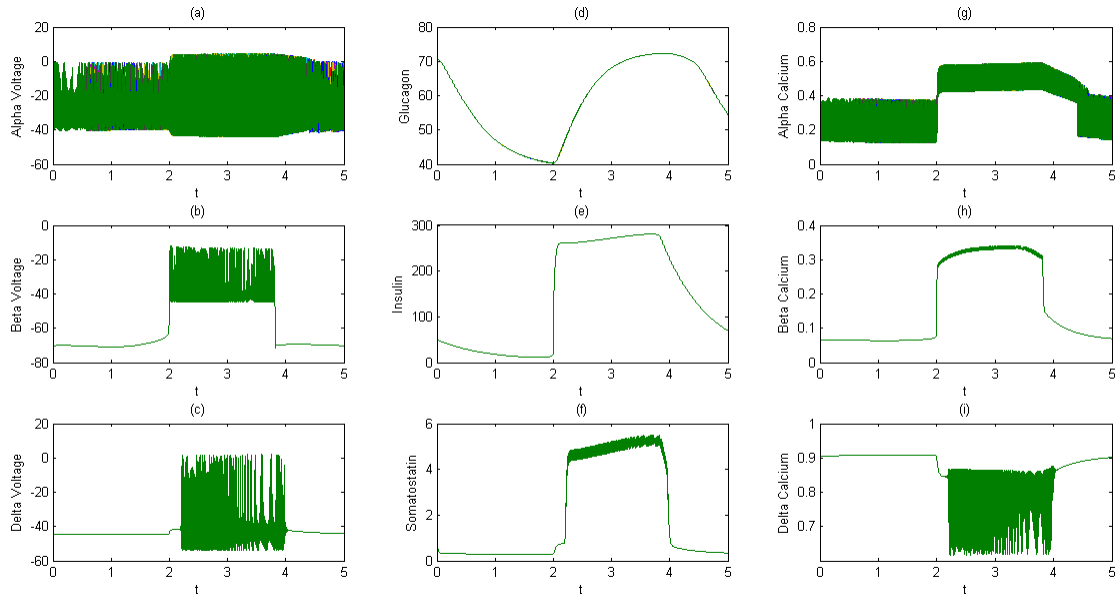


Figure 4.6: Spatial Case 3

We were also able to create a visual representation of the flow of the secreted hormone through the discretized islet.

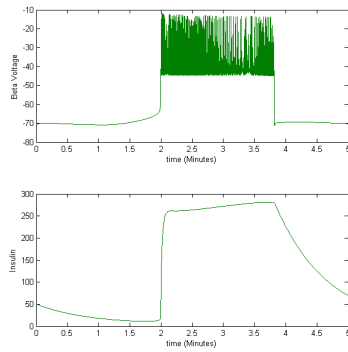
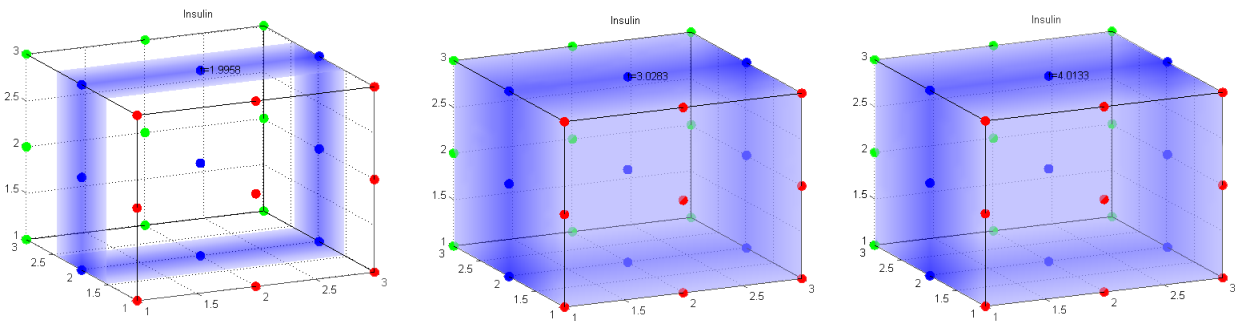


Figure 4.7: Compartmentalized Case 4



At the exact time when the beta cell voltage spikes, the amount of insulin greatly in-

creases, as can be confirmed by the 3D model at that point in time.

## 4.5 Spatial Case 4

A similar process for the Spatial analogue of the Compartmentalized Case 4. There are some noteworthy observations here as well. The alpha voltage greatly increases after the first beta spike. Until that point, the voltage oscillations have much smaller amplitudes. The delta spike also only occurs after the beta spike. Another key thing to note is the spectrum of color in our graph. We actually ended up graphing each cell a different color, to see if the cells were acting differently.

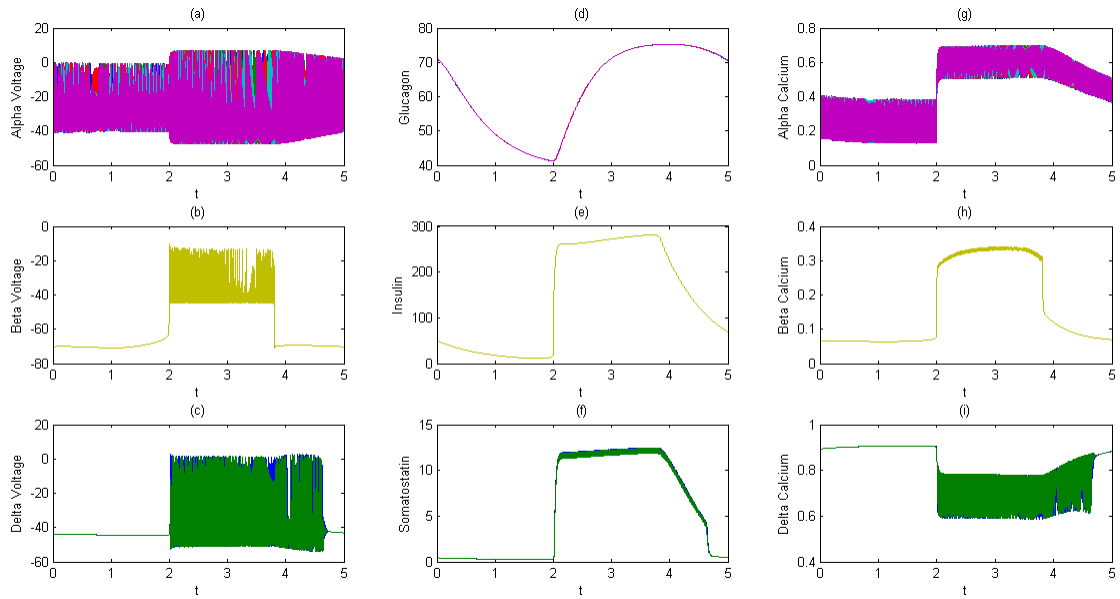


Figure 4.8: Spatial Case 4

In the compartmentalized model, we saw very little color variation, as expected. Since all cells received the same hormonal inputs, they were all acting the same. However, now that the cells are in different point in space, they receive different amounts of insulin and somatostatin, resulting in multiple cells acting heterogeneously, especially- as can be seen from our graphs- the alpha cells. We investigate paracrine interaction's effects on alpha cell heterogeneity in the next subsection.

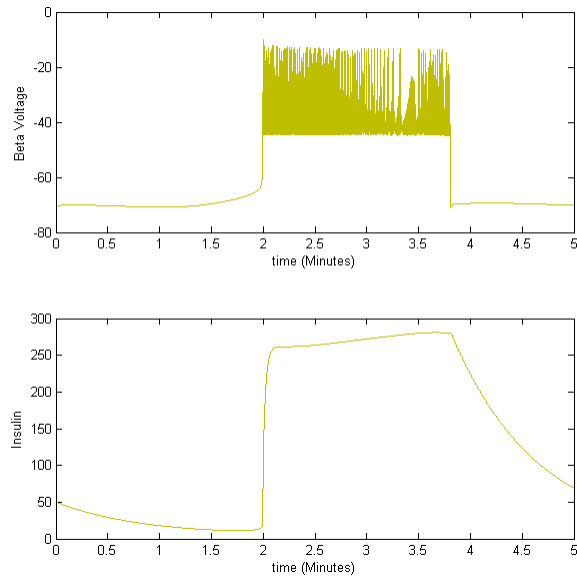
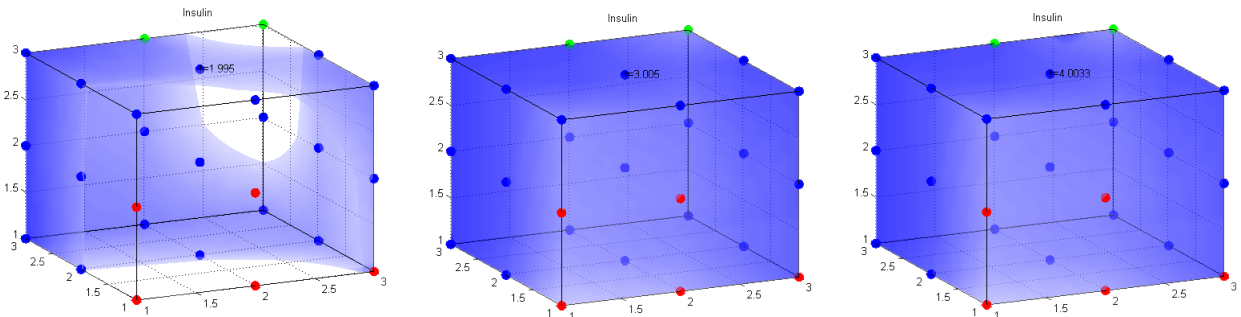


Figure 4.9: Compartmentalized Case 4



We also did a similar visual simulation of insulin secretion. We found that the insulin spread much more rapidly in to the cell, since the distribution contained much more beta cells.

## 4.6 Paracrine Interactions Cure Alpha Cell Heterogeneity

We were able to simulate heterogeneity in alpha cells with and without paracrine coupling. This was done in order to see if paracrine coupling could tame this alpha cell heterogeneity. These two simulations were ran on two  $3 \times 3 \times 3$  cube islets. For the averaged 9:9:9 cell distribution islet we assigned  $G_{K(ATP)} = 26.5 * Dza + 0.04$  to four alpha cells and  $G_{K(ATP)} = 32Dza + 0.04$  to 5 alpha cells. The non-coupled case shows a different in oscillation frequency between the heterogeneous cells. This is shown by the lack of overlap in the two voltage plots. However, when we account for the paracrine effects on the alpha cells they start to exhibit a more similar behavior. We can see this by the increase in overlap of the cell voltages. We then ran the same simulation with the mouse percentage distribution islet. We assigned  $G_{K(ATP)} = 26.5 * Dza + 0.04$  to 3 alpha cells and  $G_{K(ATP)} = 32 * Dza + 0.04$  to two alpha cells. The voltage oscillations in the Non-Coupled islet also exhibit a lack of

overlap. However, when the alpha cells are coupled with beta and delta cells there is an increase in overlap, which means the alpha cells begin to behave more similarly. A difference between this Mouse islet and the 9:9:9 case is that the mouse islet exhibit longer period of maximum voltage oscillation.

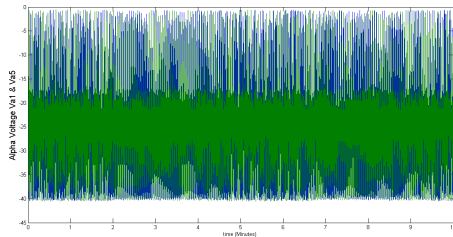


Figure 4.10: Heterogeneous 9:9:9 Islet with No Coupling

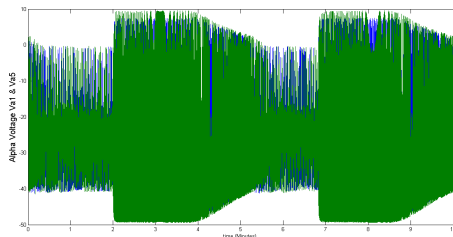


Figure 4.11: Heterogeneous 9:9:9 Islet with Coupling

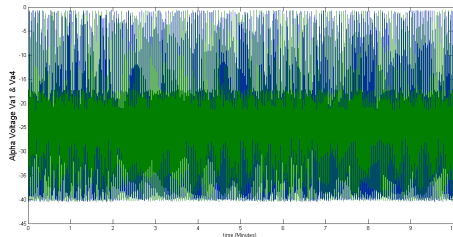


Figure 4.12: Heterogeneous Mouse Islet with no Coupling

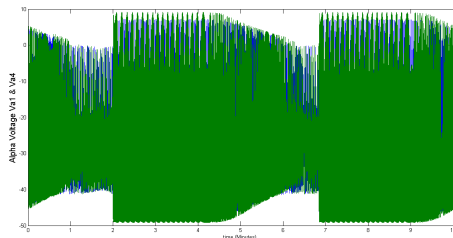


Figure 4.13: Heterogeneous Mouse Islet with Coupling

## 5 Conclusion

In producing our computational model of a pancreatic islet we have gained a better understanding in how islet size and cell distribution can affect cell behavior. We were able to

properly scale the Tri-Hormone model to a 3x3x3 cubic islet. We also successfully implemented a model in which the user is able to determine cell arrangement. This was done in order to simulate different cell proportions, specifically a mouse islet percentage, in which we were able to observe a different cell behavior than the Tri-Hormone Model. Spatial aspects of an islet were also taken into consideration by modeling secretion with a heat secretion equation. We were also able to run simulations testing the effects of paracrine coupling on alpha cell heterogeneity.

When we scaled the Tri-Hormone Model from a three-cell model to a twenty-seven-cell model we were able to replicate cell behavior. After averaging the amount of secretion detected by each cell the voltages and secretion for each cell emulated that which was found in the Tri-Hormone model. We then compare this result with a mouse islet cell distribution. When more beta cells are incorporated into an islet as in the mouse islet we see a change in behavior in the alpha and delta cells. We see an increase in the oscillation period for these cells, which could be due to the increase in insulin in the islet.

We were also able to notice that paracrine effects have a taming quality in relation to alpha cell heterogeneity. When we did not account for paracrine coupling and assigned different  $GK(ATP)$  values for our alpha cells we observed a different behavior between cells. However, when we accounted for the effect that beta and delta cells have on alpha cells, the alpha cells began to act more homogeneously.

Moving forward in this project it would be interesting to simulate larger islets. This would be done in order to test if scaling an islet affects cell behavior. Creating larger islet would also allow the user to simulate more complex and realistic cell arrangements.

It would also be interesting to run simulations in which the distance between cells was not one unit in the (i,j,k) direction. This could be done in order to observe how certain cells behave when surrounded by a specific type of cell. For example, how an alpha cell that is surrounded by beta cells behaves compared to an alpha cell in which its neighbors vary.

## Acknowledgments

These results were obtained as part of the REU Site: Interdisciplinary Program in High Performance Computing ([www.umbc.edu/hpcreu](http://www.umbc.edu/hpcreu)) in the Department of Mathematics and Statistics at the University of Maryland, Baltimore County (UMBC) in Summer 2014. This program is funded jointly by the National Science Foundation and the National Security Agency (NSF grant no. DMS-1156976), with additional support from UMBC, the Department of Mathematics and Statistics, the Center for Interdisciplinary Research and Consulting (CIRC), and the UMBC High Performance Computing Facility (HPCF). HPCF is supported by the U.S. National Science Foundation through the MRI program (grant nos. CNS-0821258 and CNS-1228778) and the SCREMS program (grant no. DMS-0821311), with additional substantial support from UMBC. Co-author Kendall Queen was supported, in part, by the UMBC National Security Agency (NSA) Scholars Program through a contract with the NSA. Graduate assistant Teresa Lehair was supported during Summer 2014 by UMBC.

## References

- [1] Statistics About Diabetes, June 2014.
- [2] Gemma Gearhart, Shuai Jiang, Thomas J. May, Jane Pan, Samuel Khuvis, Matthias K. Gobbert, Bradford E. Peercy, and Arthur Sherman. Investigating oscillation loss in computational islets. *High Performance Computing Facility*, HPCF-2013-14, August 2013.
- [3] Ivan Queseda, Eva Tuduri, Cristina Ripoll, and Angel Nadal. Physiology of the pancreatic  $\alpha$ -cell and glucagon secretion: role in glucose homeostasis and diabetes. *Journal of Endocrinology*, 199:5–19, March 2008.
- [4] Margaret Watts and Arthur Sherman. Modeling the Pancreatic  $\alpha$ -Cell: Dual Mechanisms of Glucose Suppression of Glucagon Secretion. *Biophysical Journal*, 106, February 2013.
- [5] Margaret Watts and Arthur Sherman. Modeling Paracrine Interactions in Pancreatic Islets, July 2014.
- [6] Margaret Watts and Arthur Sherman. Tri-Hormone Model. June 2014.